

Surface Reactions and Electronic Structure of Carboxylic Acid Porphyrins Adsorbed on TiO₂(110)

Daniel Wechsler, Priscila Vensaus, Nataliya Tsud, Hans-Peter Steinrück, Ole Lytken,* and Federico J. Williams*

Cite This: *J. Phys. Chem. C* 2021, 125, 6708–6715

Read Online

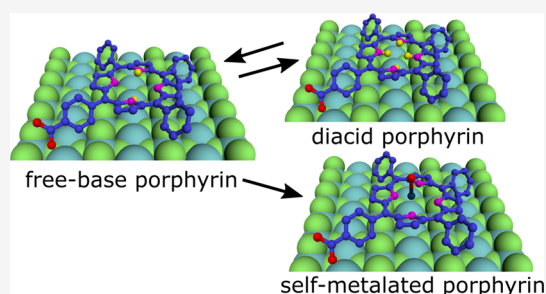
ACCESS |

Metrics & More

Article Recommendations

Supporting Information

ABSTRACT: We studied the coverage- and temperature-dependent proton transfer and self-metalation reactions of tetraphenylporphyrin molecules containing a carboxyl functional group (MCTPP) on rutile TiO₂(110) surfaces. Furthermore, we also determined changes in the molecular geometric and electronic structures as a function of coverage and temperature. The investigation was carried out by means of synchrotron radiation X-ray photoelectron spectroscopy and near-edge X-ray absorption fine structure measurements. We found that at a coverage of 0.2 ML, most MCTPP molecules adsorb with the iminic nitrogen atoms protonated; at 0.5 ML, a decrease in the proportion of protonated molecules is observed; and at a monolayer coverage, most molecules are not protonated. Raising the temperature to above 500 K, where hydroxyl groups recombine to desorb as water, causes a decrease in the number of protonated porphyrin molecules. In roughly the same temperature range, we start to observe the self-metalation of the free-base molecules, which produces flat-lying titanyl porphyrin molecules on the TiO₂(110) surface. This reaction is found to be coverage dependent: For 0.2 ML, it starts above 450 K, and for 1.0 ML, temperatures above 650 K are needed. Metalation shifts the surface state located in the semiconductor band gap to lower energies. Our results suggest that protonation and self-metalation depend on the proximity of the macrocycle to the surface and show that metalation modifies the molecular occupied and vacant electronic states.



INTRODUCTION

Functional materials composed of organic films on metal oxide substrates are of pivotal importance in prominent technologies such as photovoltaics,¹ molecular electronics,² gas sensing,³ and molecular catalysis.⁴ Their behavior can be optimized, modifying the structural and electronic properties of both the oxide and the molecular film. Using porphyrin molecules as building blocks of functional organic films provides a flexible and robust means of tuning their structural and electronic properties.⁵ Indeed, modifying the metal center and/or the peripheral groups in the macrocycle allows for controlling the chemical and electronic properties of the molecule.⁶ Furthermore, different anchoring groups can be easily incorporated in the molecular structure, enabling covalent bonding to different substrates.⁷ Therefore, some of the emerging technologies in the field are based on the interaction of porphyrin molecules with oxide surfaces, where dye-sensitized solar cells serve as the principal example.⁸ These devices are based on the adsorption of light-harvesting porphyrin molecules on titania surfaces. The anchoring and adsorption geometry of the molecules are critical points limiting charge transfer and thus the overall light-to-electron conversion efficiency.⁹ Therefore, extensive fundamental research has been recently carried out to understand the

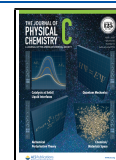
bonding and interaction of porphyrin molecules with TiO₂ surfaces.

The ideal rutile TiO₂(110) surface is composed of alternating rows of twofold-coordinated O²⁻ ions and fivefold-coordinated Ti⁴⁺ ions, and it is the most thermodynamically stable face of the oxide.¹⁰ This semiconducting surface exhibits oxygen vacancies, which can be partly filled after water adsorption to form hydroxyl species.¹¹ At a very low coverage, porphyrin molecules adsorb flat lying onto oxygen vacancies due to the localized interaction between the macrocycle and the vacancy.^{12,13} STM measurements show that carboxyl-substituted Zn porphyrins are adsorbed with the macrocycle parallel to the TiO₂(110) surface at low coverages.¹⁴ Furthermore, on the 2 × 1 reconstructed TiO₂(110) surface, flat-lying molecules co-exist with tilted molecules, and the proportion of the latter increases with coverage.¹⁵ Increasing the molecular coverage is known to affect the adsorption geometry of the molecule. NEXAFS measurements

Received: February 7, 2021

Revised: March 10, 2021

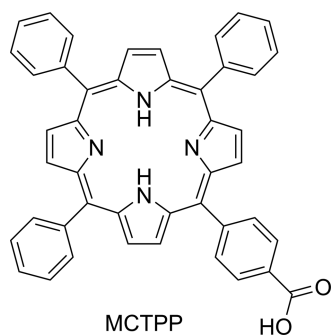
Published: March 23, 2021



suggest that Zn protoporphyrins adsorbed on $\text{TiO}_2(110)$ undergo a flat lying-to-tilted adsorption geometry transition as the molecular coverage increases.¹⁶ The number and position of phosphonic acid and carboxylic acid peripheral groups are also known to modify the adsorption geometry of porphyrin molecules on $\text{TiO}_2(110)$ surfaces.^{17,18} Free-base porphyrins adsorbed on $\text{TiO}_2(110)$ and $\text{TiO}_2(110)-2 \times 1$ surfaces can undergo reactions with co-deposited Ni metal atoms to form metalloporphyrins.^{19,20} In addition, the molecule can also experience different reactions with the $\text{TiO}_2(110)$ surface. The iminic nitrogen atoms of free-base porphyrins are known to protonate after adsorption at room temperature.²¹ Moreover, increasing the temperature enables the self-metalation reaction where a titanyl group is removed from the $\text{TiO}_2(110)$ surface and inserted into the macrocycle.^{22,23} In our previous work, we showed that the temperature onset for self-metalation of carboxyl-substituted tetraphenyl porphyrins was dependent on molecular coverage.²⁴ This suggested an adsorption geometry change from flat lying to tilted with coverage. Recently, we showed that on some oxide surfaces, self-metalation can take place even below room temperature.²⁵

In this work, we investigated the interaction of 5-(4-carboxyphenyl)-10,15,20-triphenylporphyrin (MCTPP, see Scheme 1) molecules with the rutile $\text{TiO}_2(110)$ surface. We

Scheme 1. Chemical Structure of 5-(4-Carboxyphenyl)-10,15,20-triphenylporphyrin



studied the protonation and self-metalation reactions as a function of coverage and temperature using X-ray photoelectron spectroscopy (XPS). Furthermore, we determined the position of the porphyrin electronic states with respect to the semiconductor bands as a function of temperature. We employed near-edge X-ray absorption fine structure (NEXAFS) measurements to estimate the molecular orientation as a function of coverage and temperature. Our results highlight the importance of molecular coverage and orientation in the surface chemistry of porphyrin molecules.

METHODS

All measurements were performed at the Materials Science beamline at Elettra Synchrotron in Trieste, Italy. Its end station has a base pressure of 2×10^{-10} mbar and is equipped with an SPECS Phoibos 150 hemispherical energy analyzer. The crystal temperature was measured reproducibly with K-type thermocouples attached to the sample plate and not directly touching the crystal. Therefore, the measured values during heating overestimate the actual sample temperature. This was corrected by measuring some temperature values with a pyrometer and assuming a linear deviation over the whole temperature range. Here, we note that this procedure could

result in an overestimation of the high temperature values. All XP spectra were aligned to the Ti $2p_{3/2}$ peak of 459.0 eV (the shifts required were less than 0.3 eV). Prior to each experiment, the $\text{TiO}_2(110)$ crystal was cleaned by several cycles of sputtering and annealing. The cleanliness was checked with XPS. Besides small traces of carbon (<1% of a monolayer), no impurities were found. MCTPP was deposited by evaporation in UHV from a Knudsen cell, while the clean $\text{TiO}_2(110)$ single-crystal sample was kept at room temperature. To ensure that the deposited molecules were indeed intact 5-(4-carboxyphenyl)-10,15,20-triphenylporphyrin molecules, we confirmed the carbon-to-nitrogen-to-oxygen ratios of the deposited multilayers. The C/N/O ratio of the deposited multilayers was calculated from Al $K\alpha$ XPS integrated signals using tabulated atomic sensitivity factors. For coverage calculations, a porphyrin monolayer reference was created by heating at 600 K for 10 min to desorb multilayers; the corresponding coverage is denoted as 1 ML (see Figure S1 in the Supporting Information).

The photon flux at the N K-edge was recorded with a gold mesh and found to be almost constant. In contrast, due to carbon impurities on the gold mesh, the photon flux at the C K-edge had to be measured by following the photoemission intensity of the Ti 3p peak of the clean $\text{TiO}_2(110)$ surface as a function of photon energy. With this method, the lowest photon flux in the C K-edge region was found to be only 30% of the highest flux in the same region, an effect caused by carbon impurities on the X-ray optics. The C and N K-edges were measured by following the C and N KLL Auger intensities (250–270 and 360–385 eV, respectively) as a function of photon energy. This method is sensitive to photoemission features traveling through the regions of the Auger lines, and we corrected this using a cleanup procedure described elsewhere.²⁶

RESULTS AND DISCUSSION

Figure 1a shows the N 1s XPS, and Figure 1b shows the valence band spectra of the clean $\text{TiO}_2(110)$ surface and after the adsorption of 0.2, 0.5, and 1 ML and multilayers of MCTPP.

The N 1s multilayer spectrum shows the characteristic shape for metal-free porphyrins with two peaks of equal intensity at 399.8 and 397.8 eV due to the aminic ($-\text{NH}-$) and the iminic ($=\text{N}-$) nitrogen atoms in the macrocycle, respectively (green curves).²² Furthermore, the spectrum shows two barely visible shake-up satellite peaks at a higher binding energy (magenta curves). In the 0.2, 0.5, and 1 ML spectra, the high binding energy component at 399.8 eV has a larger intensity, indicating the presence of a new contribution at this binding energy. This additional peak has been previously observed after the adsorption of metal-free porphyrins on $\text{TiO}_2(110)$ ^{21,22} and was assigned to protonated porphyrins formed after the iminic nitrogen atoms capture protons. A possible proton source could be the hydroxyl groups present on the $\text{TiO}_2(110)$ surface. In the doubly protonated form (MCTPP^{2+}), all nitrogen atoms are equivalent and therefore give only one XPS contribution at 399.8 eV, whereas in the monoprotinated form (MCTPP^+), 3 N atoms would give an XPS peak at 399.8 eV, and 1 N atom would give a peak at 397.8 eV. Note that flat-lying 2HTPP molecules at low coverages are fully protonated after adsorption on $\text{TiO}_2(110)$.²² For simplicity, we will assume the doubly protonated form when discussing the degree of protonation, although both forms are very likely

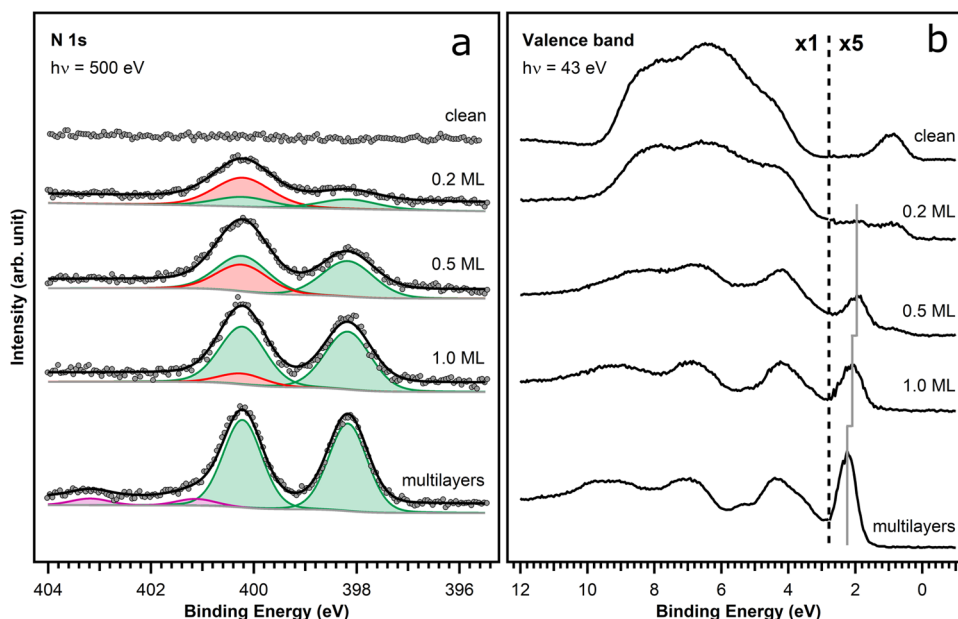


Figure 1. (a) N 1s XPS and (b) valence band spectra of the clean $\text{TiO}_2(110)$ surface and after deposition of 0.2, 0.5, and 1 ML and multilayers of MCTPP.

present. Interestingly, the proportion of protonated molecules (red curve) in Figure 1a decreases with an increasing coverage. To be more specific, the percentages of diacid molecules are 60, 27, and 9% for coverages of 0.2, 0.5, and 1 ML, respectively. If we assume that capturing a proton requires the macrocycle center to be in the proximity of the surface, then the observed decrease in the degree of protonation with an increasing molecular coverage could be due to a change in the adsorption geometry of the molecule. Indeed, NEXAFS measurements of carboxyl-substituted Zn protoporphyrin adsorbed on $\text{TiO}_2(110)$ have shown flat-lying molecules at low coverages and tilted molecules at monolayer coverages.¹⁶ This reported behavior is in line with our XPS data and with the NEXAFS measurements discussed below.

The O 1s XPS spectra (see Figure S2 in the Supporting Information) indicate that the carboxylic acid functional group is completely deprotonated when adsorbing 1 ML of MCTPP on the $\text{TiO}_2(110)$ surface, suggesting the formation of a covalent carboxylate bond to the surface. At a submonolayer coverage where the O 1s XPS spectra are largely dominated by the substrate peak, the molecular contribution is hardly distinguished, and thus no conclusion regarding bonding to the surface can be drawn.

Figure 2a shows the C K-edge and Figure 2b the N K-edge NEXAFS spectra for 0.2 and 1 ML and multilayers of MCTPP deposited on $\text{TiO}_2(110)$. The spectra corresponding to 0.2 and 1 ML were measured at normal (0°) and grazing (80°) photon incidence. Normal photon incidence implies that the electric field of the horizontally polarized radiation is parallel to the surface, whereas grazing photon incidence implies that the electric field forms an angle of 80° with respect to the surface.

The C K-edge NEXAFS spectra show a first peak at 284.5 eV, which is attributed to an electronic transition from a C 1s to a π^* orbital of the porphyrin ring.²⁷ The second peak at 285.6 eV is due to transitions from a C 1s to a π^* orbital of the phenyl rings with some contribution from the porphyrin ring.²⁸ The 0.2 ML spectra show a π^* transition at 287.5 eV that is not present in the 1 ML and multilayer spectra. These last two

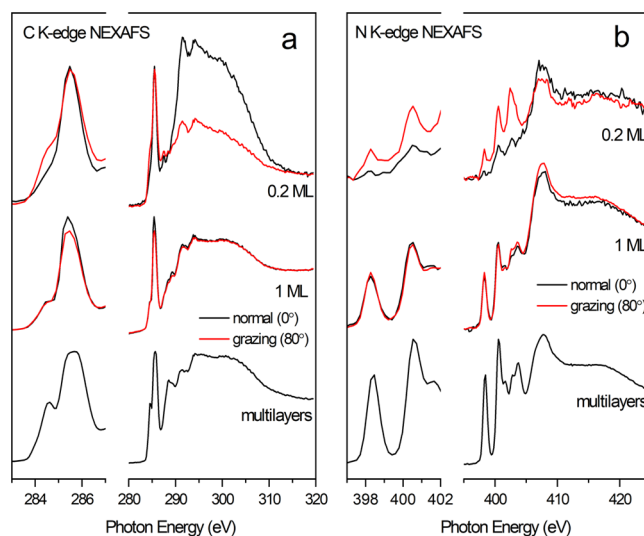


Figure 2. (a) C K-edge and (b) N K-edge NEXAFS spectra measured at normal and grazing photon incidence angles for 0.2 and 1 ML of MCTPP adsorbed on $\text{TiO}_2(110)$.

spectra show a small peak at 288.5 eV, which is not present in the 0.2 ML spectra. Finally, the broad peaks from 292 to 305 eV are due to several electronic transitions from C 1s to different σ^* orbitals.²⁸

The N K-edge NEXAFS spectra show peaks at 398.5 and 400.5 eV, which are assigned to transitions from the iminic N 1s and the aminic N 1s to the lowest lying π^* orbital from the porphyrin ring, respectively.²⁹ These peaks are followed by three π^* transitions in the 1 ML and multilayer spectra and two π^* transitions in the 0.2 ML spectrum. Finally, the spectra contain broad peaks above 408 eV due to electronic transitions to σ^* orbitals.²⁹

Note that all the transitions observed in the 1 ML C and N K-edges NEXAFS spectra are also present in the corresponding multilayer spectra. However, the spectrum corresponding to 0.2 ML shows some differences most likely related to the

fraction of protonated molecules also observed in XPS, see Figure 1a. The change in the intensity ratios of the first two π^* resonances in the N K-edge spectra are consistent with the change observed in XPS, but the strong resonance at 402.3 eV could be related to a new electronic transition specific for the protonated molecule.

The intensity of the NEXAFS features depends on the orientation of the molecular transition dipole moment relative to the electric field of the incoming radiation. When the electric field vector is parallel to the transition dipole moment, the maximum intensity is observed. On the other hand, when the electric field vector is perpendicular to the transition dipole moment, the transition is forbidden. Therefore, the dependence of the absorption intensity on the photon incidence angle gives information about the average molecular orientation.³⁰ In order to extract information regarding the adsorption geometry in twofold-symmetry substrates, it is necessary to measure the absorption intensity as a function of both the polar and azimuthal photon incidence angles.^{18,30} Here, we measured the NEXAFS spectra as a function of the polar angle for one azimuthal orientation preventing us from extracting precise adsorption angles. However, we know that carboxylic acid and phosphonic acid mono-functionalized tetraphenylporphyrin molecules exhibit no azimuthal dependence when adsorbed on TiO₂(110).^{17,18} Therefore, if we assume that MCTPP molecules adsorbed on TiO₂(110) are not aligned in any particular azimuthal direction, then we can speculate on the molecular orientation. Under this hypothesis, we note that in both the C and N K-edge NEXAFS spectra corresponding to 0.2 ML, the π^* transitions into the macrocycle molecular orbitals are very intense at grazing angles (red spectra) and almost vanish at normal incidence (black spectra). This indicates that the macrocycle is flat-lying at 0.2 ML in line with room-temperature STM measurements for Zn-MCTPP on TiO₂(110) that show flat-lying molecules at low coverages.¹⁴ The behavior at a 1 ML coverage is quite different. In this case, the spectra displayed in Figure 2a,b show no linear dichroism, that is, neither the π^* nor the σ^* resonances are a function of the polar incidence angle. This observation indicates either a disordered monolayer or a monolayer consisting of tilted molecules at the angle in which there is no dependence with the photon polar incidence angle (54.7°).³⁰ Recently, we have used angle-resolved photoelectron spectroscopy to study the growth of Co-MCTPP on TiO₂(110), and we found that monolayer deposition results in a disordered layer that grows in three dimensions.³¹ Thus, the NEXAFS measurements corresponding to the MCTPP monolayer could indicate a disordered monolayer. Hence, under the assumption of no preferred azimuthal orientation, our NEXAFS data suggest that as we go from low coverages to monolayer coverages, the number of molecules with the macrocycle tilted away from the surface increases as there is a transition from flat-lying molecules to a disordered layer. This is in line with the adsorption geometry transition from mostly flat lying to mostly upright standing observed in the past for carboxylic acid-functionalized porphyrin molecules adsorbed on oxide surfaces.^{16,32}

Figure 1b shows the valence band spectra measured as a function of molecular coverage using a photon energy of 43 eV. The top spectrum corresponding to the clean TiO₂(110) rutile surface shows a broad O 2p band from 3.4 to 10 eV below the Fermi level, in excellent agreement with previous reports.³³ Furthermore, the spectrum also shows a band-gap

state about 0.9 eV below the Fermi level, which has been assigned to the presence of oxygen vacancies or titanium interstitials.³⁴ The bottom spectrum corresponds to MCTPP multilayers on TiO₂(110). It only shows the occupied molecular states of MCTPP since substrate electrons are fully attenuated by the thick molecular film. The spectrum shows at least five peaks due to emission from one or several molecular orbitals each. The HOMO is in the band gap of the substrate, 2.2 eV below the Fermi level. It corresponds to a molecular orbital with a high electronic density at the macrocycle.³⁵ The following state at 4.4 eV corresponds to a molecular orbital with a high electronic density in the phenyl groups.³⁵ While these states can be seen in the spectra for 1 and 0.5 ML, only the HOMO band is clearly visible in the 0.2 ML spectrum because the other states overlap with the substrate bands in this case. We note that the HOMO state is shifted to lower binding energy values in the 0.2 and 0.5 ML spectra relative to the positions in the 1 ML spectrum. This could be due to the different adsorption geometry and the resulting variation in the degree of protonation for these two coverages. Finally, we note that the intensity of the band-gap state is quenched as the coverage increases. We attribute this to the attenuation of the photoelectrons by the overlying molecular layer.

The N 1s XPS spectra were measured after the adsorption of 0.2 (Figure 3a), 0.5 (Figure 3b), and 1 ML (Figure 3c) of MCTPP on TiO₂(110) as a function of temperature. As previously reported for free-base porphyrin molecules, increasing the temperature results in self-metalation, as indicated by the progressive appearance of a new XPS signal

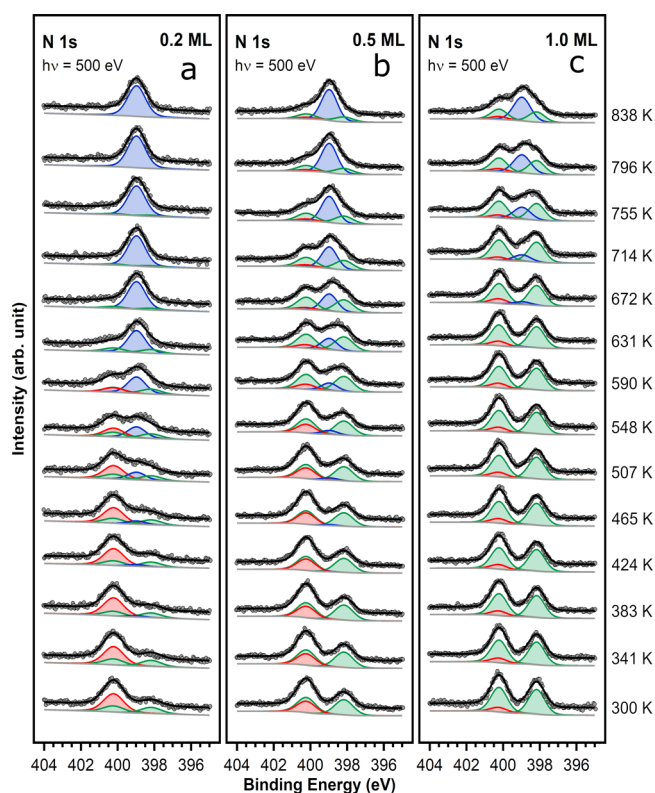


Figure 3. N 1s XPS spectra measured after adsorption of (a) 0.2, (b) 0.5, and (c) 1 ML of MCTPP molecules on TiO₂(110) as a function of temperature. Note that the spectra were measured after annealing at the specified temperature for 10 min and cooling to 300 K.

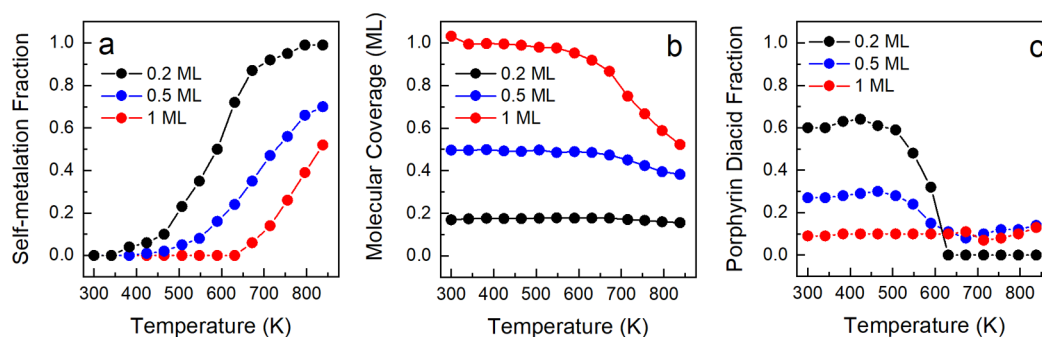


Figure 4. (a) Fraction of self-metalated molecules, (b) molecular coverage, and (c) fraction of protonated molecules as a function of temperature corresponding to an initial adsorption of 0.2, 0.5, and 1 ML MCTPP on $\text{TiO}_2(110)$.

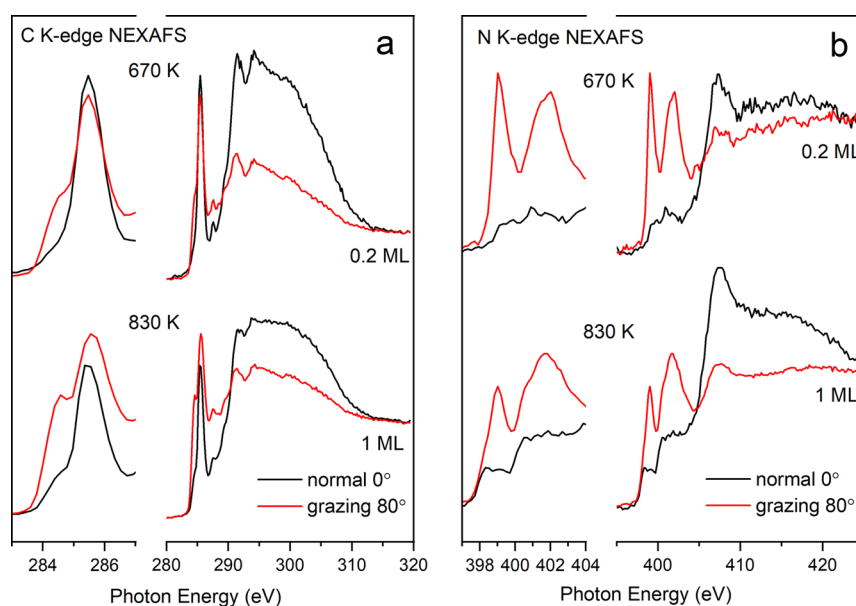


Figure 5. (a) C and (b) N K-edges NEXAFS spectra at 670 and at 830 K corresponding to 0.2 and 1 ML of MCTPP molecules adsorbed on $\text{TiO}_2(110)$, respectively, at grazing (red) and normal (black) photon incidence.

at 398.3 eV (fitted in blue).^{22–24} It is proposed that in this chemical reaction, a titanyl group from the surface is inserted into the macrocycle center, releasing two hydrogen atoms and making all four nitrogen atoms equivalent. Our data provides clear evidence that raising the temperature increases the degree of MCTPP self-metalation. Notably, we find that as the initial molecular coverage increases, a higher temperature is needed to enable the self-metalation reaction. This behavior is evident from Figure 4a, which shows the percentage of self-metalated molecules as a function of temperature for the three different initial coverages.

Figure 4a shows that the temperature-induced self-metalation of 0.2 and 0.5 ML starts at around 400–500 K. However, the self-metalation reaction of 1 ML of MCTPP molecules can only proceed above 650 K. We propose that the reason for this temperature difference is that at higher coverages, molecules form a compact layer with the macrocycle away from the surface. Before the reaction can proceed, the macrocycle needs to get into closer proximity with the surface. Figure 4b shows that the surface coverage of an initial 1 ML MCTPP layer (red) starts decreasing at ~ 600 K. This observation is in agreement with the coverage reduction observed for MCTPP adsorbed on TiO_2 nanoparticles above 573 K.³⁶ It implies that some molecules are desorbing or that the molecular monolayer

is dewetting. In either case, the effect would be to create space near MCTPP molecules, enabling the macrocycle to move in closer proximity to the surface, enabling self-metalation (see Figure 5a,b below). We note that the MCTPP adsorbed on TiO_2 nanoparticles suffers from decarboxylation above 623 K and that the loss of the functional group does not drive self-metalation.³⁶

Figure 4c shows the effect of temperature in the fraction of protonated molecules (note that the fraction was calculated with respect to the number of free-base molecules). At 1 ML, the degree of protonated molecules is always below 0.1 and remains essentially constant with temperature. However, at 0.2 and 0.5 ML, there is a clear decrease in the proportion of protonated molecules above 500 K. Notably, at 500 K, there is water desorption from the recombination of surface hydroxyl groups on $\text{TiO}_2(110)$.³⁷ This should drive the chemical equilibrium of the protonation reaction toward the free-base molecule, decreasing the fraction of protonated molecules as observed.

Figure 5a shows the C K-edge and Figure 5b the N K-edge NEXAFS spectra of 0.2 and 1 ML of MCTPP adsorbed on $\text{TiO}_2(110)$ and annealed to 670 K (0.2 ML) and to 830 K (1 ML) to induce self-metalation for grazing (red) and normal (black) photon incidence. Due to the different degree of

metalation for 0.2 ML (100%) at 670 K and 1 ML (50%) at 830 K, the corresponding NEXAFS spectra exhibit slight differences in relation to the room-temperature spectra (Figure 2a,b). Notwithstanding, the spectra display well-defined π^* and σ^* resonances. Note that the 0.2 ML N K-edge spectra show the same main features as those measured for titanyl tetraphenyl porphyrin adsorbed on Ag(111);³⁸ however, there are small differences as adsorption on Ag(111) distorts the macrocycle. For 0.2 ML, both the C K-edge and N K-edge spectra at 670 K show the same angular dependence as the RT spectra: the π^* resonances originating at the macrocycle have a maximum intensity at grazing incidence, whereas the σ^* transitions have a higher intensity at normal incidence. If we assume no preferential azimuthal orientation, then this implies that at 0.2 ML, the adsorption geometry of self-metalated MCTPP remains with the macrocycle mostly parallel to the surface when the temperature is increased to 670 K. A similar angular dependence is observed in the 830 K C and N K-edge NEXAFS spectra, corresponding to an initial 1 ML coverage. The π^* resonances originating in the macrocycle in both the C K-edge and N K-edge spectra show a pronounced increase when the incidence angle changes from normal to grazing, suggesting a flat-lying macrocycle. This indicates that the compact and disordered monolayer at room temperature changes to a flat-lying metalated layer at 830 K. Recall that at this temperature, some MCTPP molecules desorbed (Figure 4b), thus creating space for tilted molecules in the otherwise compact layer to move closer to the surface. This is in line with the interpretation of the XPS data discussed above, suggesting that self-metalation requires the macrocycle to be near the surface to proceed successfully.

The self-metalation reaction changes the molecular electronic states. The valence band spectra as a function of temperature for initial coverages of 0.2 (Figure 6a), 0.5 (Figure 6b), and 1 ML (Figure 6c) were measured with a 43 eV photon energy. As the temperature increases and the self-metalation reaction takes place, the position of the HOMO shifts to a lower binding energy as indicated by the blue line. At a high temperature, the HOMO is located at 1.76 eV below the Fermi level for all coverages. This suggests that the insertion of the titanyl group into the macrocycle shifts the HOMO to lower binding energies in agreement with predicted and observed changes when metalating free-base porphyrin molecules.^{6,39} Finally, we note that in the 1 ML spectra, the oxygen defect state located at 0.9 eV below the Fermi level reappears around 750 K. This could be due to the generation of new oxygen vacancies⁴⁰ or to the reduction of surface coverage observed at this temperature (see Figure 4b), which should diminish the attenuation of the substrate signals.

CONCLUSIONS

MCTPP molecules adsorb with the macrocycle mostly parallel to the surface at low coverages. This adsorption geometry enables protonation of the iminic nitrogen atoms probably by surface hydroxyl groups. Raising the temperature to 500 K, where water desorption from the recombination of surface hydroxyl groups takes place, causes a decrease in the proportion of protonated molecules. At the same temperature, self-metalation begins to occur, where a titanyl group is inserted into the macrocycle center. The fully metalated layer remains flat lying on the surface as the temperature is raised to 670 K. Increasing the molecular coverage at room temperature decreases the degree of protonation. Furthermore, it is

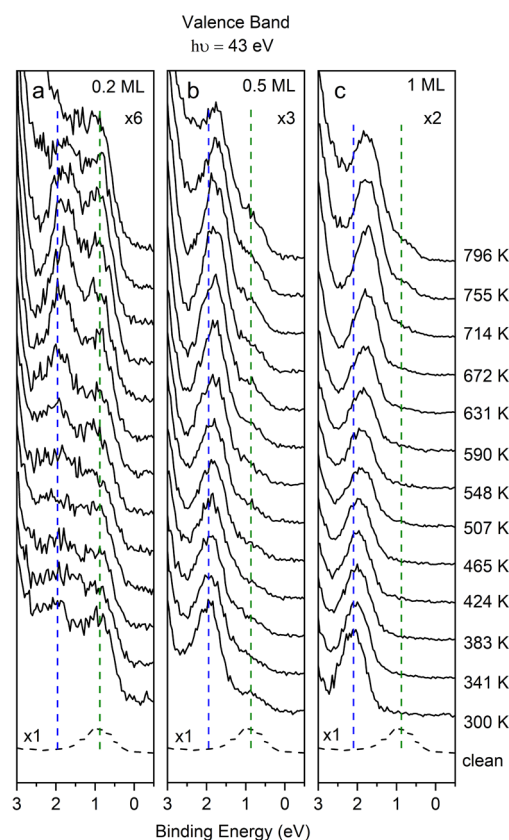


Figure 6. Valence band spectra as a function of temperature after adsorption of (a) 0.2, (b) 0.5, and (c) 1 ML of MCTPP. The spectra corresponding to the clean $\text{TiO}_2(110)$ surface are shown in broken lines. Note that the spectra were measured after annealing at the specified temperature for 10 min and cooling to 300 K.

necessary to decrease the molecular coverage, by raising the temperature, for the self-metalation reaction to occur. We propose that the self-metalation reaction takes place after the macrocycle moves closer to the surface as NEXAFS indicates a more flat-lying geometry after raising the temperature. Self-metalation causes a change in the molecular electronic structure, shifting the highest occupied molecular orbital closer to the Fermi edge. Hence, our results show that self-metalation is coverage dependent and that an adsorption configuration with the macrocycle in the proximity to the surface is required for the reaction to take place.

ASSOCIATED CONTENT

Supporting Information

The Supporting Information is available free of charge at <https://pubs.acs.org/doi/10.1021/acs.jpcc.1c01133>.

Monolayer calibration and O 1s XPS data (PDF)

AUTHOR INFORMATION

Corresponding Authors

Ole Lytken – *Lehrstuhl für Physikalische Chemie II, Universität Erlangen-Nürnberg, Erlangen 91058, Germany;*
 orcid.org/0000-0003-0572-0827; Email: ole.lytken@fau.de

Federico J. Williams – *Departamento de Química Inorgánica, Analítica y Química Física, Facultad de Ciencias Exactas y Naturales, INQUIMAE-CONICET, Universidad de Buenos*

Aires, Buenos Aires C1428EHA, Argentina; orcid.org/0000-0002-6194-2734; Email: fwilliams@qi.fcen.uba.ar

Authors

Daniel Wechsler – Lehrstuhl für Physikalische Chemie II, Universität Erlangen-Nürnberg, Erlangen 91058, Germany

Priscila Vensaus – Departamento de Química Inorgánica, Analítica y Química Física, Facultad de Ciencias Exactas y Naturales, INQUIMAE-CONICET, Universidad de Buenos Aires, Buenos Aires C1428EHA, Argentina; orcid.org/0000-0002-3859-5578

Nataliya Tsud – Department of Surface and Plasma Science, Faculty of Mathematics and Physics, Charles University, Prague 18000, Czech Republic; orcid.org/0000-0001-7439-7731

Hans-Peter Steinrück – Lehrstuhl für Physikalische Chemie II, Universität Erlangen-Nürnberg, Erlangen 91058, Germany; orcid.org/0000-0003-1347-8962

Complete contact information is available at: <https://pubs.acs.org/10.1021/acs.jpcc.1c01133>

Notes

The authors declare no competing financial interest.

ACKNOWLEDGMENTS

This project was financially supported by the Deutsche Forschungsgemeinschaft (DFG) within the Research Unit FOR 1878 funCOS – Functional Molecular Structures on Complex Oxide Surfaces by the Agencia Nacional de Promoción de la Investigación, el Desarrollo Tecnológico y la Innovación (PICT-2018-03276) and by the Universidad de Buenos Aires (20020190100028BA). P.V. acknowledges the scholarship from Bayerisches Hochschulzentrum für Lateinamerika (BAYLAT). F.J.W. thanks DFG for financial funding through the Mercator Fellowship. CERIC-ERIC consortium and Czech Ministry of Education, Youth and Sports (projects LM2018116 and CZ.02.1.01/0.0/0.0/18_046/0015962) are acknowledged for financial support.

REFERENCES

- (1) O'Regan, B.; Grätzel, M. A Low-Cost, High-Efficiency Solar Cell Based on Dye-Sensitized Colloidal TiO₂ Films. *Nature* **1991**, *353*, 737–740.
- (2) Jurow, M.; Schuckman, A. E.; Batteas, J. D.; Drain, C. M. Porphyrins as Molecular Electronic Components of Functional Devices. *Coord. Chem. Rev.* **2010**, *254*, 2297–2310.
- (3) Huang, L.; Wang, Z.; Zhu, X.; Chi, L. Electrical Gas Sensors Based on Structured Organic Ultra-Thin Films and Nanocrystals on Solid State Substrates. *Nanoscale Horiz.* **2016**, *1*, 383–393.
- (4) Zhang, W.; Jiang, P.; Wang, Y.; Zhang, J.; Zhang, P. Bottom-up Approach to Engineer Two Covalent Porphyrinic Frameworks as Effective Catalysts for Selective Oxidation. *Catal. Sci. Technol.* **2015**, *5*, 101–104.
- (5) Auwärter, W.; Écija, D.; Klappenberger, F.; Barth, J. V. Porphyrins at Interfaces. *Nat. Chem.* **2015**, *7*, 105–120.
- (6) Gottfried, J. M. Surface Chemistry of Porphyrins and Phthalocyanines. *Surf. Sci. Rep.* **2015**, *70*, 259–379.
- (7) Zhang, L.; Cole, J. M. Anchoring Groups for Dye-Sensitized Solar Cells. *ACS Appl. Mater. Interfaces* **2015**, *7*, 3427–3455.
- (8) Li, L.-L.; Diau, E. W.-G. Porphyrin-Sensitized Solar Cells. *Chem. Soc. Rev.* **2013**, *42*, 291–304.
- (9) Hart, A. S.; KC, C. B.; Gobeze, H. B.; Sequeira, L. R.; D'Souza, F. Porphyrin-Sensitized Solar Cells: Effect of Carboxyl Anchor Group Orientation on the Cell Performance. *ACS Appl. Mater. Interfaces* **2013**, *5*, 5314–5323.

(10) Diebold, U. The Surface Science of Titanium Dioxide. *Surf. Sci. Rep.* **2003**, *48*, 53–229.

(11) Bikondoa, O.; Pang, C. L.; Ithnin, R.; Murny, C. A.; Onishi, H.; Thornton, G. Direct Visualization of Defect-Mediated Dissociation of Water on TiO₂(110). *Nat. Mater.* **2006**, *5*, 189–192.

(12) Inada, M.; Scifo, L.; Tanaka, S.; Grevin, B.; Suzuki, H.; Mashiko, S. Scanning Tunneling Microscopy of Porphyrin-Based Molecules on TiO₂ Surfaces. *Jpn. J. Appl. Phys., Part 1* **2006**, *45*, 2103–2105.

(13) Lackinger, M.; Janson, M. S.; Ho, W. Localized Interaction of Single Porphyrin Molecules with Oxygen Vacancies on TiO₂(110). *J. Chem. Phys.* **2012**, *137*, 234707.

(14) Zajac, L.; Olszowski, P.; Godlewski, S.; Bodek, L.; Such, B.; Jöhr, R.; Pawlak, R.; Hinaut, A.; Glatzel, T.; Meyer, E.; et al. Self-Assembling of Zn Porphyrins on a (110) Face of Rutile TiO₂—The Anchoring Role of Carboxyl Groups. *Appl. Surf. Sci.* **2016**, *379*, 277–281.

(15) Olszowski, P.; Zajac, L.; Godlewski, S.; Such, B.; Jöhr, R.; Glatzel, T.; Meyer, E.; Szymanski, M. Role of a Carboxyl Group in the Adsorption of Zn Porphyrins on TiO₂(011)-2×1 Surface. *J. Phys. Chem. C* **2015**, *119*, 21561–21566.

(16) Rienzo, A.; Mayor, L. C.; Magnano, G.; Satterley, C. J.; Ataman, E.; Schnadt, J.; Schulte, K.; O'Shea, J. N. X-Ray Absorption and Photoemission Spectroscopy of Zinc Protoporphyrin Adsorbed on Rutile TiO₂(110) Prepared by in Situ Electrospray Deposition. *J. Chem. Phys.* **2010**, *132*, No. 084703.

(17) Fernández, C. C.; Wechsler, D.; Rocha, T. C. R.; Steinrück, H.-P.; Lytken, O.; Williams, F. J. Adsorption of Phosphonic-Acid-Functionalized Porphyrin Molecules on TiO₂(110). *J. Phys. Chem. C* **2019**, *123*, 10974–10980.

(18) Fernández, C. C.; Wechsler, D.; Rocha, T. C. R.; Steinrück, H.-P.; Lytken, O.; Williams, F. J. Adsorption Geometry of Carboxylic Acid Functionalized Porphyrin Molecules on TiO₂(110). *Surf. Sci.* **2019**, *689*, 121462.

(19) Wang, C.; Fan, Q.; Hu, S.; Ju, H.; Feng, X.; Han, Y.; Pan, H.; Zhu, J.; Gottfried, J. M. Coordination Reaction between Tetraphenylporphyrin and Nickel on a TiO₂(110) Surface. *Chem. Commun.* **2014**, *50*, 8291–8294.

(20) Wang, C.; Fan, Q.; Han, Y.; Martínez, J. I.; Martín-Gago, J. A.; Wang, W.; Ju, H.; Gottfried, J. M.; Zhu, J. Metalation of Tetraphenylporphyrin with Nickel on a TiO₂(110)-1×2 Surface. *Nanoscale* **2016**, *8*, 1123–1132.

(21) Lovat, G.; Forrer, D.; Abadia, M.; Dominguez, M.; Casarin, M.; Rogero, C.; Vittadini, A.; Floreano, L. Hydrogen Capture by Porphyrins at the TiO₂(110) Surface. *Phys. Chem. Chem. Phys.* **2015**, *17*, 30119–30124.

(22) Köbl, J.; Wang, T.; Wang, C.; Drost, M.; Tu, F.; Xu, Q.; Ju, H.; Wechsler, D.; Franke, M.; Pan, H.; et al. Hungry Porphyrins: Protonation and Self-Metalation of Tetraphenylporphyrin on TiO₂(110)-1×1. *ChemistrySelect* **2016**, *1*, 6103–6105.

(23) Lovat, G.; Forrer, D.; Abadia, M.; Dominguez, M.; Casarin, M.; Rogero, C.; Vittadini, A.; Floreano, L. On-Surface Synthesis of a Pure and Long-Range-Ordered Titanium(IV)-Porphyrin Contact Layer on Titanium Dioxide. *J. Phys. Chem. C* **2017**, *121*, 13738–13746.

(24) Wechsler, D.; Fernández, C. C.; Steinrück, H.-P.; Lytken, O.; Williams, F. J. Covalent Anchoring and Interfacial Reactions of Adsorbed Porphyrins on Rutile TiO₂(110). *J. Phys. Chem. C* **2018**, *122*, 4480–4487.

(25) Wechsler, D.; Fernández, C. C.; Tariq, Q.; Tsud, N.; Prince, K. C.; Williams, F. J.; Steinrück, H.-P.; Lytken, O. Interfacial Reactions of Tetraphenylporphyrin with Cobalt-Oxide Thin Films. *Chemistry* **2019**, *25*, 13197–13201.

(26) Lytken, O.; Wechsler, D.; Steinrück, H.-P. Removing Photoemission Features from Auger-Yield NEXAFS Spectra. *J. Electron Spectrosc. Relat. Phenom.* **2017**, *218*, 35–39.

(27) Cudia, C. C.; Vilmercati, P.; Larciprete, R.; Cepek, C.; Zampieri, G.; Sangaletti, L.; Pagliara, S.; Verdini, A.; Cossaro, A.; Floreano, L.; et al. Electronic Structure and Molecular Orientation of

a Zn-Tetra-Phenyl Porphyrin Multilayer on Si(111). *Surf. Sci.* **2006**, *600*, 4013–4017.

(28) Diller, K.; Klappenberger, F.; Marschall, M.; Hermann, K.; Nefedov, A.; Wöll, C.; Barth, J. V. Self-Metalation of 2H-Tetraphenylporphyrin on Cu(111): An x-Ray Spectroscopy Study. *J. Chem. Phys.* **2012**, *136*, No. 014705.

(29) Polzonetti, G.; Carravetta, V.; Iucci, G.; Ferri, A.; Paolucci, G.; Goldoni, A.; Parent, P.; Laffon, C.; Russo, M. V. Electronic Structure of Platinum Complex/Zn-Porphyrinato Assembled Macrosystems, Related Precursors and Model Molecules, as Probed by X-Ray Absorption Spectroscopy (NEXAFS): Theory and Experiment. *Chem. Phys.* **2004**, *296*, 87–100.

(30) Stöhr, J.; Outka, D. A. Determination of Molecular Orientations on Surfaces from the Angular Dependence of Near-Edge x-Ray-Absorption Fine-Structure Spectra. *Phys. Rev. B* **1987**, *36*, 7891–7905.

(31) Kataev, E.; Wechsler, D.; Williams, F. J.; Köbl, J.; Tsud, N.; Franchi, S.; Steinrück, H.-P.; Lytken, O. Probing the Roughness of Porphyrin Thin Films with X-ray Photoelectron Spectroscopy. *ChemPhysChem* **2020**, *21*, 2293–2300.

(32) Rangan, S.; Ruggieri, C.; Bartynski, R.; Martínez, J. I.; Flores, F.; Ortega, J. Densely Packed ZnTPPs Monolayer on the Rutile TiO₂(110)-(1×1) Surface: Adsorption Behavior and Energy Level Alignment. *J. Phys. Chem. C* **2016**, *120*, 4430–4437.

(33) Rangan, S.; Katalinic, S.; Thorpe, R.; Bartynski, R. A.; Rochford, J.; Galoppini, E. Energy Level Alignment of a Zinc(II) Tetraphenylporphyrin Dye Adsorbed onto TiO₂(110) and ZnO(11 $\bar{2}$ 0) Surfaces. *J. Phys. Chem. C* **2009**, *114*, 1139–1147.

(34) Yim, C. M.; Pang, C. L.; Thornton, G. Oxygen Vacancy Origin of the Surface Band-Gap State of TiO₂(110). *Phys. Rev. Lett.* **2010**, *104*, No. 036806.

(35) Giovanelli, L.; Lee, H.-L.; Lacaze-Dufaure, C.; Koudia, M.; Clair, S.; Lin, Y.-P.; Ksari, Y.; Themlin, J.-M.; Abel, M.; Cafolla, A. A. Electronic Structure of Tetra(4-Aminophenyl)Porphyrin Studied by Photoemission, UV–Vis Spectroscopy and Density Functional Theory. *J. Electron Spectrosc. Relat. Phenom.* **2017**, *218*, 40–45.

(36) Kollhoff, F.; Schneider, J.; Li, G.; Barkaoui, S.; Shen, W.; Berger, T.; Diwald, O.; Libuda, J. Anchoring of Carboxyl-Functionalized Porphyrins on MgO, TiO₂, and Co₃O₄ Nanoparticles. *Phys. Chem. Chem. Phys.* **2018**, *20*, 24858.

(37) Du, Y.; Petrik, N. G.; Deskins, N. A.; Wang, Z.; Henderson, M. A.; Kimmel, G. A.; Lyubinetsky, I. Hydrogen Reactivity on Highly-Hydroxylated TiO₂(110) Surfaces Prepared Via carboxylic Acid Adsorption and Photolysis. *Phys. Chem. Chem. Phys.* **2012**, *14*, 3066–3074.

(38) Duncan, D. A.; Deimel, P. S.; Wiengarten, A.; Paszkiewicz, M.; Casado Aguilar, P.; Acres, R. G.; Klappenberger, F.; Auwärter, W.; Seitsonen, A. P.; Barth, J. V.; et al. Bottom-Up Fabrication of a Metal-Supported Oxo–Metal Porphyrin. *J. Phys. Chem. C* **2019**, *123*, 31011–31025.

(39) Auwärter, W.; Seufert, K.; Klappenberger, F.; Reichert, J.; Weber-Bargioni, A.; Verdini, A.; Cvetko, D.; Dell'Angela, M.; Floreano, L.; Cossaro, A.; et al. Site-Specific Electronic and Geometric Interface Structure of Co-Tetraphenyl-Porphyrin Layers on Ag(111). *Phys. Rev. B* **2010**, *81*, 245403.

(40) Rogala, M.; Bihlmayer, G.; Dabrowski, P.; Rodenbücher, C.; Wrana, D.; Krok, F.; Klusek, Z.; Szot, K. Self-Reduction of the Native TiO₂(110) Surface during Cooling after Thermal Annealing – in-Operando Investigations. *Sci. Rep.* **2019**, *9*, 12563.